Journal of CO_2 Utilization 12 (2015) 62–76

Contents lists available at ScienceDirect

Journal of CO_2 Utilization

journal homepage: www.elsevier.com/locate/jcou

A comparative study of CO_2 utilization in methanol synthesis with various syngas production technologies

Minh Tri Luu[a], Dia Milani[a], Alireza Bahadori[b], Ali Abbas[a,*]

[a] School of Chemical and Biomolecular Engineering, The Univeristy of Sydney, NSW 2006, Australia
[b] School of Environment, Science and Engineering, Southern Cross University, Lismore, NSW, Australia

ARTICLE INFO

Article history:
Received 8 April 2015
Accepted 7 July 2015
Available online 8 August 2015

Keywords:
Carbon capture and utilization
Methanol
Dry methane reforming
Steam methane reforming
Methanol economy

ABSTRACT

This paper explores a possible 'methanol economy' transition strategy—a novel carbon capture and utilization (CCU) configuration for methanol (MeOH) production (CCU–MeOH). In this CCU–MeOH, the captured CO_2 is co-fed with natural gas (NG) to produce syngas suitable for MeOH synthesis. The main objective of this work is to compare two aspects, namely CO_2 emission intensity and the extent of methane reliance, of six CCU–MeOH scenarios derived from four reforming methodologies (steam methane reforming (SMR), dry methane reforming (DMR), bireforming and trireforming). Among the studied CCU–MeOH scenarios, Scenario 2 (DMR with H_2 addition) significantly outperformed the other scenarios by 12.7% and 22% on average in terms of CO_2 emission intensity and methane reliance, respectively. The outperformance of Scenario 2 in CO_2 emission intensity is found to originate from a 22% reduction in CH_4 consumption on average compared to the other scenarios. In intermediate term, Scenario 2 may provide an attractive option for transitioning into 'methanol economy' of the future.
© 2015 Elsevier Ltd. All rights reserved.

1. Introduction

Mitigating the harmful effects of greenhouse-gas (GHG) emissions such as carbon dioxide (CO_2) is a well-recognized major challenge for humankind. It is estimated that 78% of total CO_2e (CO_2 equivalent) is contributed by fossil fuel combustion and industrial processes for the period 2000–2010 [1]. Despite substantial efforts being made to mitigate GHG effects, annual CO_2e emissions increased on average about 1 Gt CO_2e per year and without additional effort to reduce CO_2e, the global surface temperature is expected to increase by 3.7 to 4.8 °C in 2100 [1].

Over the past 200 years, since the industrial revolution, energy production and industrial processes consumed an incredible amount of carbon-based fuels, which had taken millions of years to form. The CIA World Factbook projected the end for oil, natural gas and coal reserves at around 2051, 2061 and 2088, respectively [2]. In order to secure our future energy, the so-called 'methanol economy'—an application of the carbon capture and utilization (CCU) concept, proposed by Olah and Goeppert offers a sustainable alternative energy model to the current carbon-based fuel model [3]. This is because the 'methanol economy' will not only reduce and eventually eliminate the reliance on fossil fuels, but will also result in a carbon-neutral loop [4]. At the core of the 'methanol economy' is the carbon capture and utilization (CCU) idea considered to be a more promising alternative to CCS (carbon capture and sequestration) scheme. Instead of sequestering the captured CO_2, CCU proposes the utilization of this CO_2 for the production of a variety of commodity chemicals, fuels and building blocks for other products [5]. Among valuable products produced by utilizing the captured CO_2 (CCU), methanol (MeOH) has received growing interests in literature. The significance of MeOH synthesis in CCU process was comprehensively discussed by Olah and Goeppert [4].

1.1. Current status of methanol economy

In the 'methanol economy' model, methanol is synthesized by using the captured CO_2 (from power plants (PP), industrial processes and atmospheric air) and H_2 from carbon-free sources. This methanol synthesis route has been widely studied and was found to successfully abate a large amount of CO_2 [6–8] and reduce the reliance on carbon-based feeds (e.g., natural gas (NG), coal) [4]. However, a major limitation associated with this MeOH production route is the requirement of a very large amount of carbon-free hydrogen supply [7]. If that MeOH synthesis scheme is considered for global scale production in the short-term, the carbon-free hydrogen sector is unlikely to be able to satisfy the hydrogen demanded for global MeOH production [9]. Therefore, it is

* Corresponding author. Fax: +61 2 9351 2854.
E-mail address: ali.abbas@sydney.edu.au (A. Abbas).

http://dx.doi.org/10.1016/j.jcou.2015.07.001
2212-9820/© 2015 Elsevier Ltd. All rights reserved.

Nomenclature

Abbrevations and symbols

BAU	Business as usual
CCS	Carbon capture and sequestration
CCU	Carbon capture and utilization
CCU-MeOH	Carbon capture and utilization based methanol production
CO_2e	CO_2 equivalent
C-T-G	Cradle-to-gate
DMR	Dry methane reforming
DMR-MeOH	Dry methane reforming based methanol production
LCA	Life cycle assessment
MeOH	Methanol
NG	Natural gas
PCC	Post-combustion carbon capture
PO	Partial methane oxidation
PP	Power plant
R&D	Research & development
RWGS	Reverse water–gas shift
SMR	Steam methane reforming
SMR-MeOH	Steam methane reforming based methanol production
tonne/h	Tonne of material flows per hour

imperative to establish a well-planed transition strategy to switch the current MeOH production from carbon-based resources to carbon-free method inspired by the novel 'methanol economy'. This is because the transition strategy will buy us time from the depletion-day of fossil fuels by partially replacing NG with captured CO_2 as illustrated in Fig. 1. Therefore, it will aid to mitigate the harmful effects of current rapid CO_2 emissions as less consumption of NG means less CO_2 emission. Thus allowing for sustainable carbon-free hydrogen sector to grow and able to supply sufficient H_2 for novel global MeOH production. After that, MeOH can be produced from carbon-free H_2 and the captured CO_2, thus closing the carbon loop as proposed in the 'methanol economy' [3]. To the best of our knowledge, very few publications studied this MeOH production transition scheme of the 'methanol economy' (Fig. 1), in spite of its mentioned potential benefits. Most of the studies on CCU–MeOH production focused on the long term goal, i.e., producing MeOH from the captured CO_2 and carbon-free hydrogen [6–8,10,11].

One of the possible transition strategies for the 'methanol economy' is co-feeding (or utilizing) the captured CO_2 (e.g., from post-combustion carbon capture (PCC)) with NG into MeOH production processes, i.e., partially replacing CH_4 with captured CO_2 (Fig. 1). Only NG based MeOH is considered in this work since it accounts for more than 75% of MeOH production and currently is the most cost effective method among other MeOH production methods (e.g., coal, biomass, CO_2) [10,11]. Galindo-Cifre and Badr reviewed the literature on MeOH production methods and showed that the cost to produce MeOH from coal and biomass are about two and four folds, respectively compared to NG-based MeOH [11].

The proposed transition strategy will not only help to slow down the depletion rate of NG resources, but will also reduce the reliance on carbon-free hydrogen. For example, hydrogen can be obtained from CH_4 and H_2O in SMR–MeOH (steam methane reforming based MeOH production). In addition, potentially co-feeding the captured CO_2 with NG for MeOH production causes less CO_2 emission compared to a comparative conventional MeOH plant due to the reduction in NG consumption rate [12]. Milani et al. studied the utilization of captured CO_2 from a 660 MWe power plant (PP) for SMR–MeOH production and demonstrated an enhancement in CO_2 abatement by 21.9% of the studied CCU scheme (MeOH plant integrated with PP + PCC plant) compared to BAU (business as usual) scenario where PP and MeOH plants work independently [12].

Beside the SMR–MeOH route, methanol can also be synthesized from syngas produced by dry methane reforming (DMR–MeOH) (Reaction (a)) (need to adjust the syngas composition) and by two DMR derivative processes, namely bireforming (simultaneous SMR and DMR) and trireforming—a combination of simultaneous SMR, DMR and partial methane oxidation (PO) [4]. All of these reforming technologies are found to be promising candidates to be employed in the transition strategy of the 'methanol economy' as they can utilize captured CO_2 for syngas production [4,13]. Although, CCU–SMR–MeOH (Reaction (b)) have been shown to consume 25.6% less CH_4 compared to a standalone comparative MeOH plant [12], theoretically it consumes 50% extra CH_4 compared to DMR–MeOH to produce the same amount of MeOH as can be seen from Reactions (a) and (b). This is because DMR–MeOH is able to utilize more CO_2, thus reducing the demand on CH_4 as compared to SMR–MeOH. From Reaction (b), it can be seen that SMR–MeOH demands a significant amount of water, thus requiring an appropriate scheme for on-site water management [14].

$$CH_4 + CO_2 + H_2 \leftrightarrow 2CH_3OH \quad (a)$$

$$\frac{3}{2}CH_4 + \frac{1}{2}CO_2 + H_2O \leftrightarrow 2CH_3OH \quad (b)$$

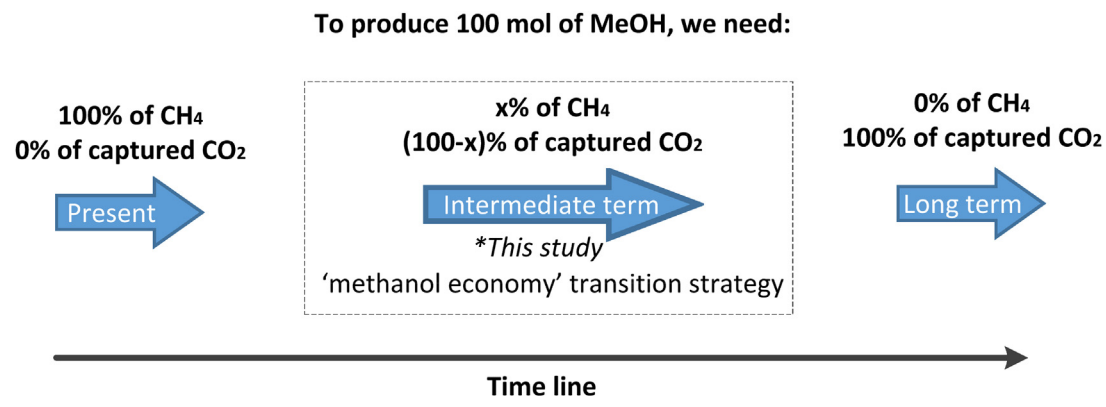

Fig. 1. Graphical presentation of the MeOH production transition from methane-based (present) to the utilized CO_2-base (sustainability situation or 'methanol economy').

If SMR- and DMR-based MeOH are placed on the time line shown in Fig. 1, DMR–MeOH show the furthest sustainability because it consumes less CH_4 and more CO_2 feeds (Reactions (a) and (b)). More importantly DMR-based MeOH requires carbon-free hydrogen (Reaction (a)). This hydrogen requirement will potentially create incentive for R&D to drive the development of a sustainable carbon-free hydrogen sector to provide sufficient carbon-free hydrogen for novel global MeOH production [15].

Presently, commercial applications of DMR are likely to be challenged by technical issues, e.g., catalyst deactivation due to coke formation. However, with significant effort for R&D, plausible progresses for DMR catalyst developments have been made [16–19]. Verykios found that the basicity support La_2O_3 on Ni catalyst can significantly stabilise the activity of the catalyst for DMR (test period was 100 h) in spite of solid carbon deposition was observed [16]. Newnham successfully optimized the performance of Ni catalyst for DMR by incorporating mesoporous alumina (MAL) with different Ni loading [17]. Ni-catalysts supported on neat MCM-41 framework developed by Lovell et al. were able to stabilise in the presence of carbon accumulation during the DMR test periods [19].

Although, MeOH production based on SMR, DMR and DMR derivative processes (bireforming and trireforming) are well-known in literature, to the best of our knowledge, few studies provided comprehensive comparisons (e.g., from environmental aspect) for those MeOH production methods which promisingly can be used in the transition strategy for the novel 'methanol economy'. Lima et al. compared two CCU–MeOH alternative processes: (1) parallel DMR and DMR (DMR and SMR occur in parallel reformers), (2) series DMR and SMR (DMR and SMR occur series reformers) [20]. Lima et al. showed that alternative 1 outperformed others in terms of technical, economic and environmental viabilities [20].

In this paper, three reforming methodologies are employed (DMR and its derivative processes: bireforming and trireforming) to convert the captured CO_2 and NG to syngas suitable for MeOH synthesis. For this purpose, a 660 MWe PP coupled with a PCC plant are considered. The captured CO_2 is then sent to the reformer to produce syngas for MeOH synthesis. The CO_2 and other impurities concentration in NG are assumed to be negligible and NG stream mainly consists of purified methane. This practice of MeOH production (i.e., via utilization of captured CO_2) will reduce the consumption of methane. As a result, CO_2e emission will be less compared to a comparative conventional MeOH plant due to the fact that there is CO_2e associated with methane consumption. The syngas used in MeOH synthesis should have an appropriate composition of H_2, CO and CO_2 which is often expressed by a so-called stoichiometric number '*M*' where '*M*' is computed as in Eq. (1) [21].

$$M = \frac{n_{H_2} - n_{CO_2}}{n_{CO} + n_{CO_2}} = 2 \quad (1)$$

where '*n*' denotes total mole of syngas components. Therefore, from the mentioned DMR-based reforming technologies, five CCU–MeOH scenarios are established as follows, in order to produce syngas with stoichiometric number *M* equal to 2:

1. DMR with surplus carbon monoxide removal [22].
2. DMR with addition of hydrogen [23].
3. Bireforming [24].

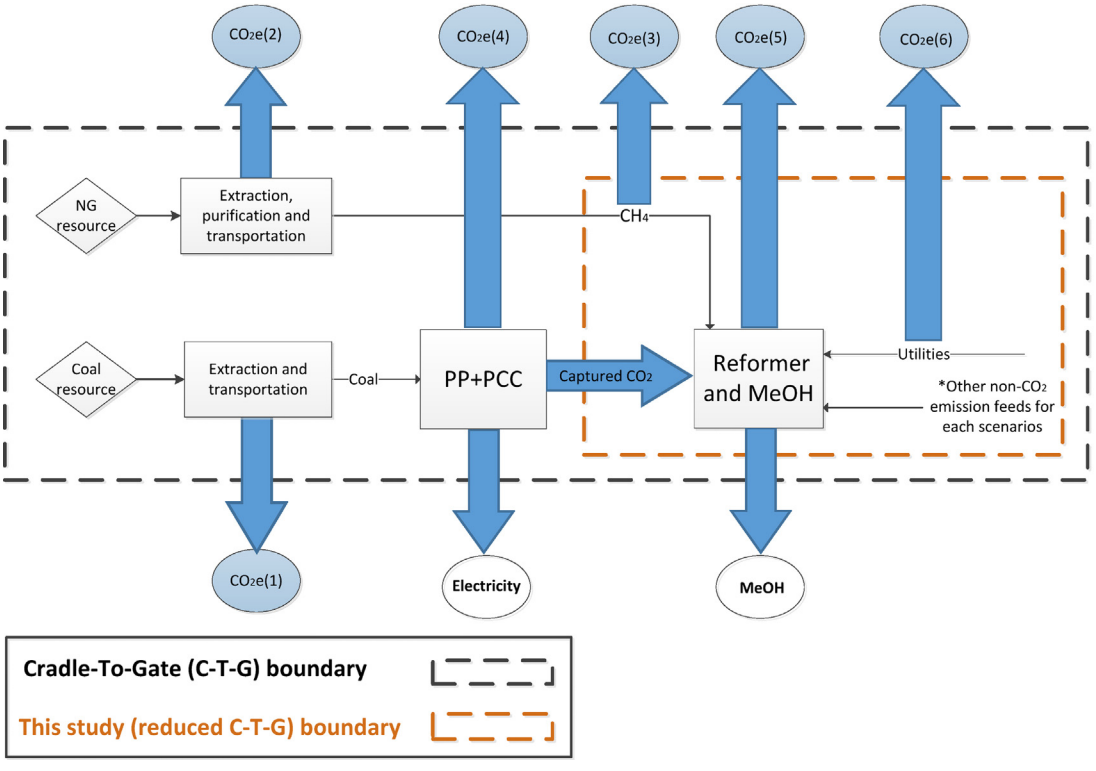

Fig. 2. Graphical presentation for the boundaries of CCU scenarios.

4. Parallel SMR and DMR [25].
5. Trireforming [26].

In addition to these five proposed scenarios (DMR-based), a SMR–MeOH scenario studied by Milani et al. and configured similar to this CCU scheme is included in the comparisons and named as SMR scenario [12]. For each scenario, a comprehensive model using Aspen Plus V8.4 (Aspentech, USA) is developed. Simulation results are used to determine total CO_2 emission, the resources (e.g., CH_4, H_2O, H_2 and O_2) and energy required to produce MeOH. Those results are used to examine two aspects of the studied CCU–MeOH scenarios, namely CO_2 emission and the extent of methane reliance.

The outcome from this study will suggest a suitable reforming technology to apply in the transitional stage of the 'methanol economy' (Fig. 1) and expected to fill the gap between the present situation of MeOH production (carbon-based) and the novel 'methanol economy' (carbon-free).

2. Methodology for evaluation of CO_2 emissions

The CCU concept is a highly attractive concept for solving the 'fossil fuel depletion' and 'global warming' problems, however, there are still variations in evaluation methodologies for CO_2 emissions [27]. In addition, without proper definition of CCU systems boundaries, the results often lack transparency [27] and processes cannot be easily comparable. Wu et al. proposed optimized syngas production processes verified in Aspen Plus subject to almost net-zero CO_2 emission [28]. However, the process boundaries in the work of Wu et al. [28] are not clearly defined; for example it is not clear whether the boundary includes the PCC, air separation unit, and biomass processes, all with potential CO_2e emissions associated with operating these processes [27]. Secondly, the source of CO_2 stream is unclear (from fossil fuels or from atmospheric air) as these sources will influence the evaluation of the CO_2 emissions [27].

Assen et al. proposed a comprehensive life cycle assessment (LCA) analysis model (Cradle-To-Gate (C-T-G)) for CCU schemes. However, the application of 'C-T-G' LCA model requires a large data bank to comprehensively account for all possible CO_2 emission sources [6]. In the present work, a systematical CO_2 emission evaluation methodology is employed; a reduced 'C-T-G' LCA model as shown in Fig. 2 is developed based on the work of Milani et al. [12]. This reduced LCA model excludes 'shared' CO_2 emission between scenarios, i.e., from the extraction, purification and transportation of raw materials (coal and CH_4) as well as from PP + PCC. Hence, it avoids the complexity of CO_2 emissions calculations for CCU scenarios, while ensuring a systematical approach. As can be seen from Fig. 2, a specific process boundary is defined in this study with three CO_2 emission points defined as follows:

- $CO_2e(3)$ is the CO_2 content in CH_4 whereby the combustion of each mole of CH_4 has potential to be converted to an equivalent mole of CO_2 (Reaction (c)). Equivalently, the potential combustion of 1 tonne of CH_4 will produce approximately 2.75 tonne of CO_2.

$$CH_4 + 2O_2 \rightarrow CO_2 + 2H_2O \quad (c)$$

- $CO_2e(5)$ is the unreacted CO_2 (or vented CO_2) in MeOH synthesis plant.
- $CO_2e(6)$ is the CO_2 emission associated with the energy consumption of utilities duty.

As a result, CO_2e associated with MeOH production can be computed from Eq. (2).

$$CO_2e \text{ for MeOH production} = CO_2e(3) + CO_2e(5) + CO_2e(6) \quad (2)$$

To determine the flow rate of $CO_2e(3)$, the feed rate of CH_4 is converted into CO_2e, thus Eq. (3) is re-written as follows:

$$CO_2e \text{ for MeOH production} = 2.75 \times (CH_4 \text{ feed rate}) + CO_2e(5) + CO_2e(6) \quad (3)$$

From Eq. (2), the CO_2 emission intensity for MeOH production ($tonne_{CO_2}/tonne_{MeOH}$) can be calculated as:

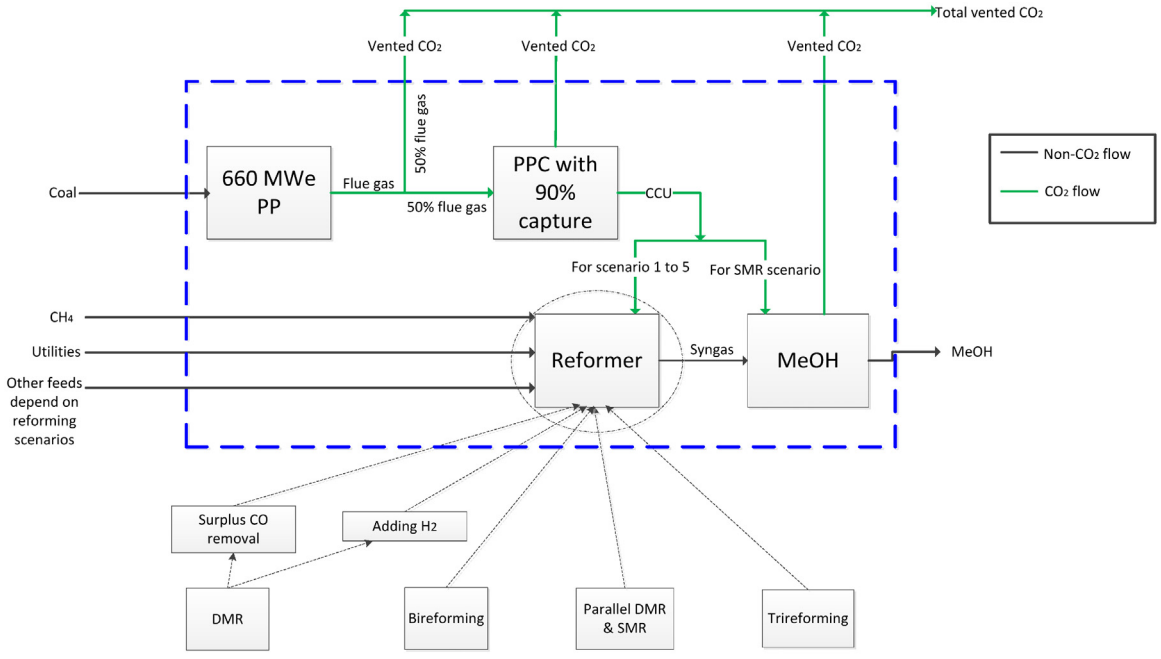

Fig. 3. Process block flow diagram for a CCU application of MeOH production (Scenarios 1–5) analysed in this study, including SMR scenario from Milani et al. [12].

$$CO_2 \text{ emission intensity} = \frac{CO_2e \text{ for MeOH production}}{\text{MeOH production}} \quad (4)$$

3. Process description

The proposed CCU structure in this study includes: a power plant (PP), post-combustion carbon capture plant (PCC), syngas production (reformer) and methanol synthesis plants (MeOH) (Fig. 3).

The reformer and MeOH plants are assumed to be integrated with an existing 660 MWe coal- fired power plant (emmits about 591 $tonne_{CO2}$/h) coupled with a PCC plant with 90% capture rate using 30 wt% MEA solvent. The PP load will often fluctuate between 50% and 100%. To stablise the operation of the PCC, reformer and MeOH synthesis plants, it is assumed that the PCC plant is designed with a capacity of 50% of PP flue gas at full load capacity. Thus, even when the PP load is down to 50%, the PCC will have the same flue gas flow uptake which is the entire mass flow out of the PP stack. The CO_2-rich stream out of PCC stack although contains trace amounts of water and other impurities (less than 1 mol%), is assumed to be carry pure CO_2 only. The total captured CO_2 and available for utilization is computed as $(50\% \times 90\% \times 591)$ 265.9 $tonne_{CO2}$/h or 6130 kmol/h. After CO_2 in the flue gas is captured and instead of being sent to sequestration it enters the reformer for syngas production, which employs a different reforming technology in each scenario. Other main feed streams (H_2O, H_2 and O_2) depending on reforming technologies are fed to the reformer. For example, in Scenario 3 (bireforming), H_2O is fed in the reformer along with the CH_4 feed, while in Scenario 2 (DMR with H_2 addition), hydrogen is fed to the reformer in addition to CH_4. At the reformer outlet, the syngas will have a stoichiometric number M approximately equal to 2 (Eq. (1)) which is appropriate for MeOH synthesis.

The structure for the present work is graphically illustrated in Fig. 4. A process model is developed in Aspen Plus for each scenario. Sensitivity analyses are subsequently carried out to determine the feed flow rates (CH_4, H_2O, O_2, H_2) in order to produce a syngas with a stoichiometric number M equal to 2 as required for efficient methanol production [21]. Once the reforming plant is able to produce syngas with a correct M value, it is linked to a validated methanol synthesis model developed by Milani et al. [12]. This methanol synthesis plant was developed based on the steady-state kinetics for CO_2 hydrogenation and reverse water gas shift reactions (RWGS) on a commercial CuO/ZnO/Al_2O_3 catalyst [29]. The results obtained from mass and energy balances of the reformer and MeOH plant simulation are used to compute the following four metrics which are used later to compare between the different scenarios:

1. $\text{Methane intensity} = \frac{CH_4 \text{feed}}{\text{MeOH produced}} \left(\text{tonne}_{CH_4}/(\text{tonne}_{MeOH_4}\right)$ (5)
2. $CO_2 \text{feed intensity} = \frac{CO_2 \text{ feed}}{\text{MeOH produced}} \left(\frac{\text{tonne}_{CO_2\text{-feed}}}{\text{tonne}_{MeOH}}\right)$ (6)
3. $\text{Energy intensity} = \frac{\text{thermal (electrical) duty}}{\text{MeOH}} \left(\frac{GJ_{\text{thermal (electrical)}}}{\text{tonne}_{MeOH}}\right)$ (7)
4. $CO_2 \text{emission intensity} \left(\frac{\text{tonne}_{CO_2}}{\text{tonne}_{MeOH}}\right)$ as calculated in (8)

4. Results

In this section, the process and Aspen Plus model for each scenario are described. In order for each scenario to produce

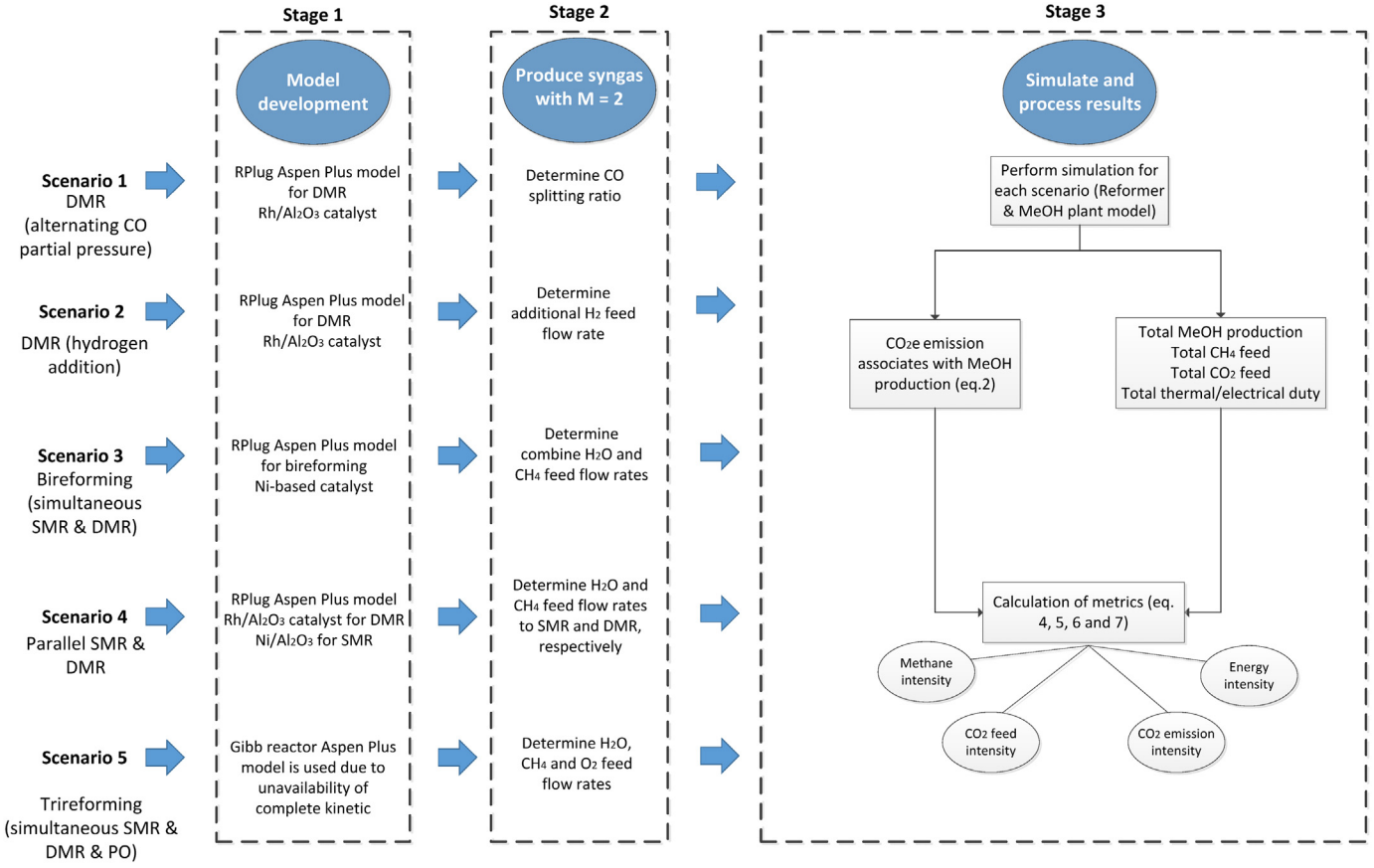
Stage 1
Stage 2
Stage 3
Model development
Produce syngas with M = 2
Simulate and process results
Scenario 1
DMR (alternating CO partial pressure)
RPlug Aspen Plus model for DMR Rh/Al2O3 catalyst
Determine CO splitting ratio
Scenario 2
DMR (hydrogen addition)
RPlug Aspen Plus model for DMR Rh/Al2O3 catalyst
Determine additional H2 feed flow rate
Scenario 3
Bireforming (simultaneous SMR & DMR)
RPlug Aspen Plus model for bireforming Ni-based catalyst
Determine combine H2O and CH4 feed flow rates
Scenario 4
Parallel SMR & DMR
RPlug Aspen Plus model Rh/Al2O3 catalyst for DMR Ni/Al2O3 for SMR
Determine H2O and CH4 feed flow rates to SMR and DMR, respectively
Scenario 5
Trireforming (simultaneous SMR & DMR & PO)
Gibb reactor Aspen Plus model is used due to unavailability of complete kinetic
Determine H2O, CH4 and O2 feed flow rates
Perform simulation for each scenario (Reformer & MeOH plant model)
CO2e emission associates with MeOH production (eq.2)
Total MeOH production
Total CH4 feed
Total CO2 feed
Total thermal/electrical duty
Calculation of metrics (eq. 4, 5, 6 and 7)
Methane intensity
Energy intensity
CO2 feed intensity
CO2 emission intensity

Fig. 4. Steps for implementation and evaluation of each scenario.

syngas with '*M*' equal to 2, a sensitivity analysis is performed. The objective here is to digest the pre-determined CO_2 stream from PCC (265.9 $tonne_{CO2}$/h) and yield syngas with a correct stoichiometric number M with minimal use of resources (H_2O, H_2, O_2). This is because increasing '*M*' above 2 (by feeding more resources) will not further enhance the effectiveness of MeOH synthesis, while only increasing the required duty in the pre-heater, reformer and at the successive compression and intercooling stages. Simulation results for each scenario are used to compute the four metrics as shown in Fig. 4. These metrics are used in the discussion section to evaluate and compare between scenarios.

Scenario 1: DMR with variable carbon monoxide partial pressure.

In this scenario, dry reforming is used for syngas production where the partial pressure of CO in the syngas at the reformer outlet is manipulated to give a stoichiometric number *M* equal to 2. As shown in Fig. 5, the methane (CH_4) and carbon dioxide (CO_2) feeds, with molar flow rate ratio (CO_2/CH_4) about 1.06 (determined thermodynamically for free solid-carbon operation at $T = 1200\,^{\circ}C$ and $P = 25$ bar), enter the heat exchanger (HX-01) to exchange the heat with the syngas at the reformer outlet (stream 5). The resulted 'hot' CH_4 and CO_2 mixture (stream 3) is preheated up to the reformer operating temperature (1200 °C). The reformer outlet (stream 5) is processed through a heat exchanger (HX-01), cooler (COOL-01) and a knock-out drum (H2ODrum), respectively. After that, it (stream 8) enters a hydrogen membrane separator (Memsep) where hydrogen is selectively removed from the syngas mixture. The CO-rich stream (stream 11) is partially sent to the mixer (MX-02) to mix with the hydrogen in stream 10 in order to give a stoichiometric number *M* equal to 2.

The reformer is modeled and optimized using the built-in RPlug model in Aspen Plus having 4 tubes packed with Rh/Al_2O_3 catalyst; each tube is 10 m in length and 0.1 m in diameter. Constant operating temperature (1200 °C) and pressure (25 bar) are specified. The model is developed based on steady-state kinetic for dry methane reforming and RWGS reactions on a Rh/Al_2O_3 catalyst. LHHW (Langmuir–Hinshelwood–Hougon–Watson) kinetic expressions for each reaction on this catalyst is provided in Richardson and Paripatyadar [30] and are rearranged into Aspen Plus compatible form as shown by Robinson [31].

To produce syngas with stoichiometric number *M* equal to 2, the partial pressure of CO in the syngas sent to the methanol synthesis plant is manipulated by adjusting the valve (V-01) as shown in Fig. 5. A sensitivity analysis is performed to determine the splitting ratio of streams 12 and 13 (Fig. 5), it is found that by blending 46 mol% of stream 11 with the hydrogen rich stream (10), the syngas sent to MeOH plant (stream 14) results in a stoichiometric number *M* equal to 2 (Fig. 6). Decreasing this splitting ratio will increase 'M', however at the cost of removing

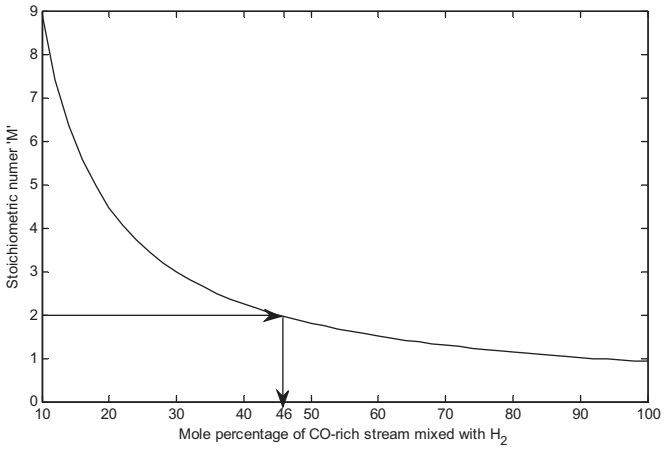

Fig. 6. Sensitivity analysis for Scenario 1 to determine the mole percentage of the CO rich stream (immediately after hydrogen separation) will mix with hydrogen and result in *M* equal to 2.

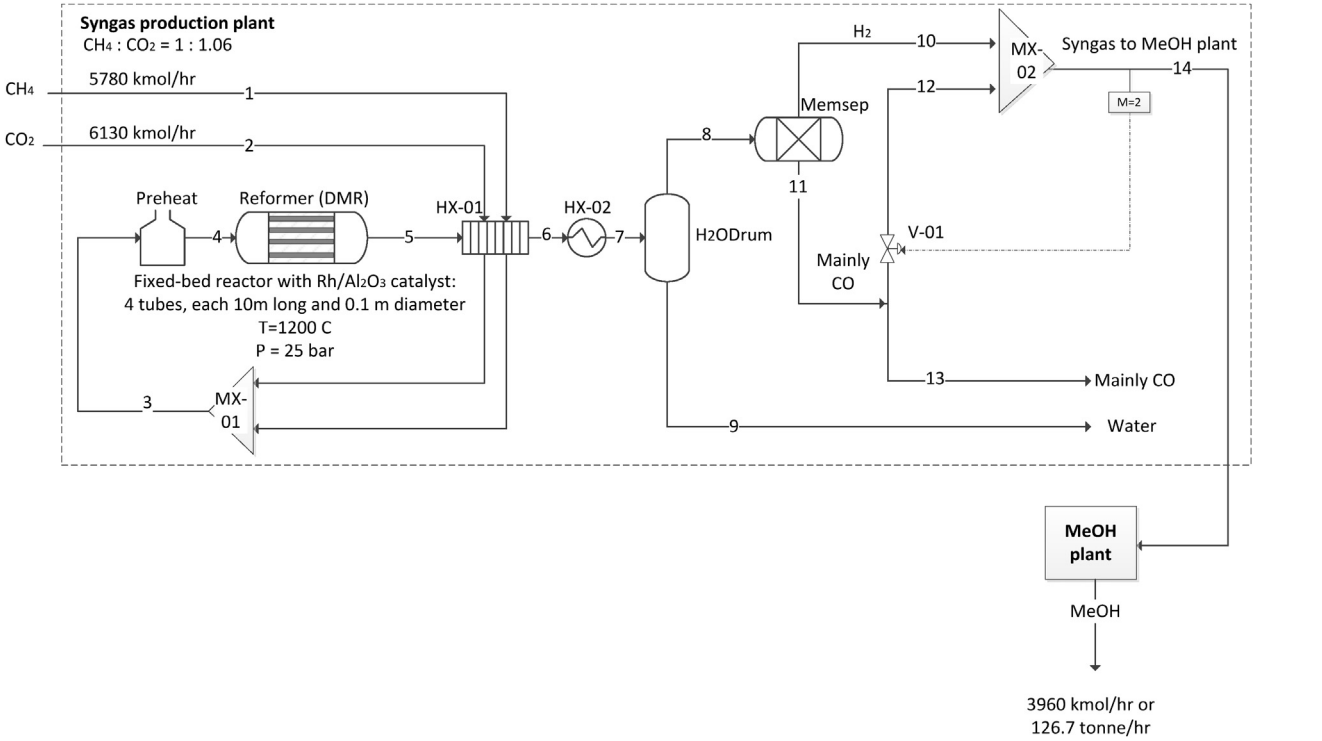

Fig. 5. Process flow diagram for the syngas production plant with CO partial pressure in the syngas to MeOH plant (stream 14) is manipulated to give a stoichiometric *M* equal to 2.

Table 1
Calculated metrics for Scenario 1.

Methane intensity	0.731	$tonne_{CH_4}/tonne_{MeOH}$
CO_2 feed intensity	2.096	$tonne_{CO_{2-feed}}/tonne_{MeOH}$
Energy intensity	16.6[b](0.734)	$GJ_{thermal(electrical)}/tonne_{MeOH}$
CO_2 emission intensity[a]	5.23	$tonne_{CO_2}/tonne_{MeOH}$

[a] Including 42% of CO_2e from the removed CO stream.
[b] For heating (6%), cooling (36%) and supplying energy to the reformer (58%).

more CO, i.e., increasing flow rate of stream 13. As a result, it will deteriorate the degree of CO_2 utilization (Table 1).

In this scenario, the reformer and MeOH plants consume 265.9 tonne of CO_2 captured from PP and a methane flow rate of 92.7 tonne/h to produce 126.8 tonne/h of MeOH. The surplus CO stream leaves the system at 181.3 tonne/h and consists of 97 wt% of CO (175.8 tonne/h) and trace amount of H_2, CO_2 and CH_4 (totally 3 wt %). In practical application, this surplus CO-rich stream can be utilized for higher hydrocarbon synthesis via Fischer–Tropsh routes. Using the simulation results in Table 9, four metrics shown in Fig. 4 are computed (using Eqs. (5)–(8)) and reported in: Table 1

Scenario 2: Adding hydrogen from carbon-free sources (e.g., solar water splitting process).

The process flow diagram of this scenario is shown in Fig. 7. It can be seen that to make '*M*' equal to 2, additional hydrogen from carbon-free source (e.g., solar water splitting process) is mixed with the syngas (stream 10). Similar to the Scenario 1, the DMR reformer in this scenario is modeled and optimized using the RPlug reactor built-in Aspen Plus having 4 tubes, each being 10 m in length and 0.1 m in diameter. The DMR reaction kinetics of an Rh/Al_2O_3 catalyst as reported by Richardson and Paripatyadar are used to model the RPlug reactor [30]. A sensitivity test is performed to determine the least hydrogen feed rate to accommodate the pre-determined CO_2 feed and give '*M*' equal to 2. The result shows that 12,710 kmol/h (25.4 tonne/h) of hydrogen is needed. Increasing the H_2 feed rate (i.e., make '*M*' larger than 2) will not further enhance the efficiency of MeOH synthesis, while only increasing the cost to supply H_2. In comparison, using the same CH_4 and CO_2 feed rates (similar to Scenario 1) will produce more MeOH (278.8 tonne/h) in this scenario. This is because an external source of hydrogen is fed to the system, thus resulting in most of the C atoms bring used to form methanol whereas about 54 mol% of C atoms are removed in the form of CO in Scenario 1. This hydrogen stream is assumed to be supplied from a carbon-free water splitting plant, thus the associated CO_2 emission is negligible. Performing similar mass and energy balance calculations as in Scenario 1, key results for this scenario are reported in Table 10. Using those results, four metrics shown in Fig. 4 are calculated (using Eqs. (5)–(8)) and reported in Table 2.

Scenario 3: Simultaneous SMR and DMR (bireforming)

This scenario (Fig. 9) applies the concept of bireforming (simultaneous SMR and DMR in one reformer) into syngas production for methanol synthesis. Water, methane and carbon dioxide are fed into one reactor (Reformer) where simultaneous steam reforming and DMR reactions occur on catalyst's pellets (e.g., Ni-based catalyst). In order to produce syngas with *M* equal to 2, both methane (stream 1) and water (stream 3) feed rates are manipulated to determine suitable combination feed rates as shown in Fig. 8. The syngas (stream 8) after water elimination in

Table 2
Calculated metrics for Scenario 2.

Methane intensity	0.333	$tonne_{CH_4}/tonne_{MeOH}$
CO_2 feed intensity	0.954	$tonne_{CO_{2-feed}}/tonne_{MeOH}$
Energy intensity	12.3[a](1.05)	$GJ_{thermal(electrical)}/tonne_{MeOH}$
CO_2 emission intensity	1.72	$tonne_{CO_2}/tonne_{MeOH}$

[a] For heating (7.5%), cooling (50%) and supplying energy to the reformer (42.5%).

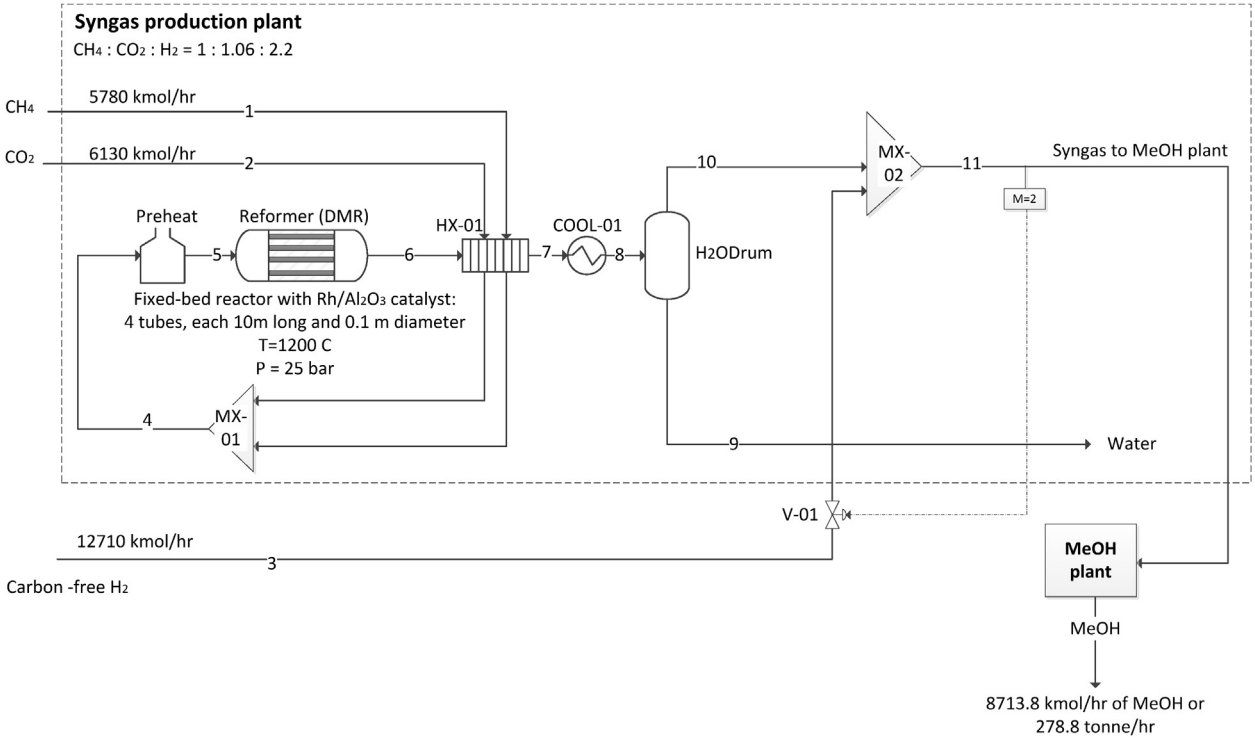

Fig. 7. Process flow diagram for syngas production plant using DMR and hydrogen from carbon-free source (stream 3) is mixed with the syngas (stream 10) to give syngas (stream 11) with a stoichiometric *M* equal to 2.

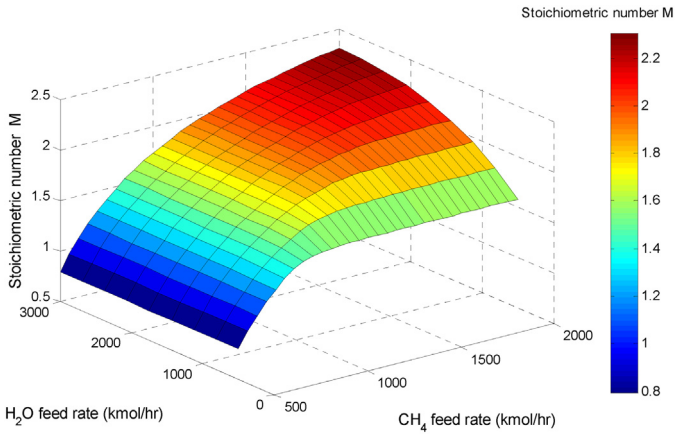

Fig. 8. The effect of H_2O and CH_4 feed rates on the stoichiometric M in Scenario 3.

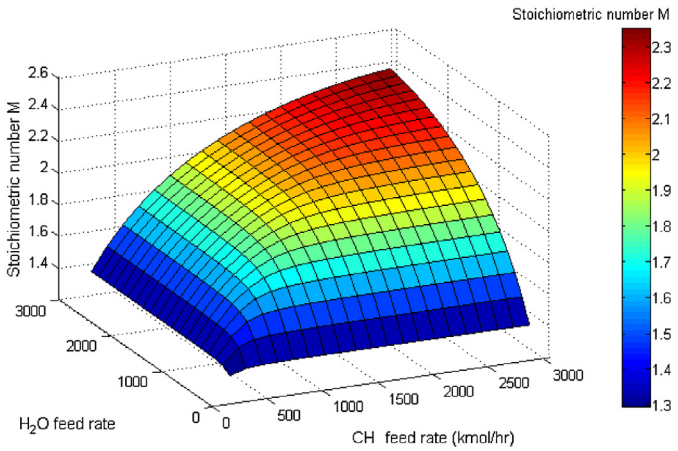

Fig. 10. Variations of stoichiometric M at different CH_4 and H_2O feed rates in Scenario 4.

Table 3
Calculated metrics for Scenario 3.

Methane intensity	0.412	$tonne_{CH_4}/tonne_{MeOH}$
CO_2 feed intensity	0.373	$tonne_{CO_{2-feed}}/tonne_{MeOH}$
Energy intensity	12.4[a](0.623)	$GJ_{thermal(electrical)}/tonne_{MeOH}$
CO_2 emission intensity	1.907	$tonne_{CO_2}/tonne_{MeOH}$

[a] For heating (9.5%), cooling (43.5%) and supplying energy to the reformer (47.1%).

the knock-out drum (H2ODrum) with a stoichiometric number M equal to 2 and is sent to the MeOH synthesis plant. It is found that the minimum CH_4 and H_2O feed rates that can digest the pre-determined CO_2 and yield a stoichiometric number M equal to 2 are 18,330 kmol/h and 14,375 kmol/h, respectively.

The bireforming reactor is modeled and optimized using the RPlug model in Aspen Plus which consists of 4 tubes, each being 10 m in length and 0.1 m in diameter. Reaction kinetics input to the RPlug model are based on Shahkarami [32] in which the author used kinetics from a Ni/Al_2O_3 catalyst to present SMR reaction [33]. Whereas for DMR reaction, Shahkarami [16] employed the kinetics of DMR reaction on a Ni/La_2O_3 catalyst as reported by Verykios [32]. The kinetic expressions are re-arranged in accordance with the LHHW formula built-in Aspen Plus. The methanol production capacity for this scenario is 713.3 tonne/h with the consumptions of 294 tonne/h of methane and 265.9 tonne/h of carbon dioxide. Results for mass and energy balance are shown in Table 11 and used to perform the calculation for the metrics as done in Scenario 1 and 2. The results are reported in Table 3.

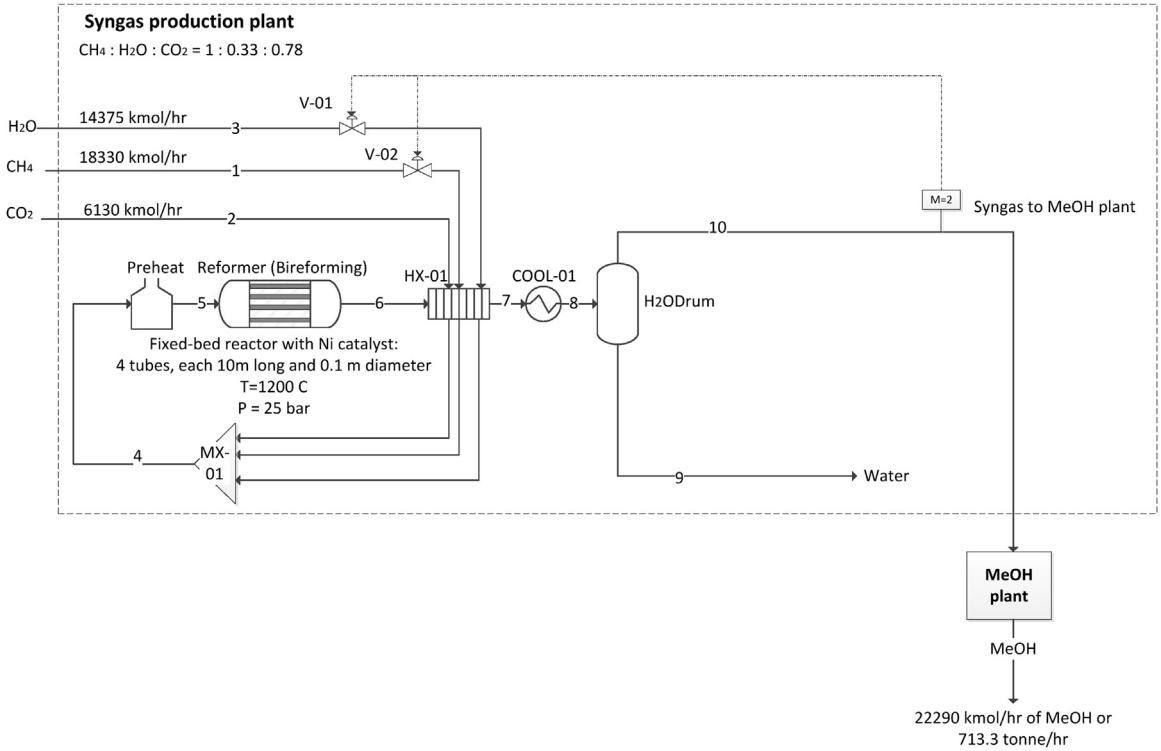

Fig. 9. Process flow diagram for the syngas production plant employing bireforming technology in the reformer to produce syngas (stream 10) with M equal to 2 suitable for MeOH synthesis.

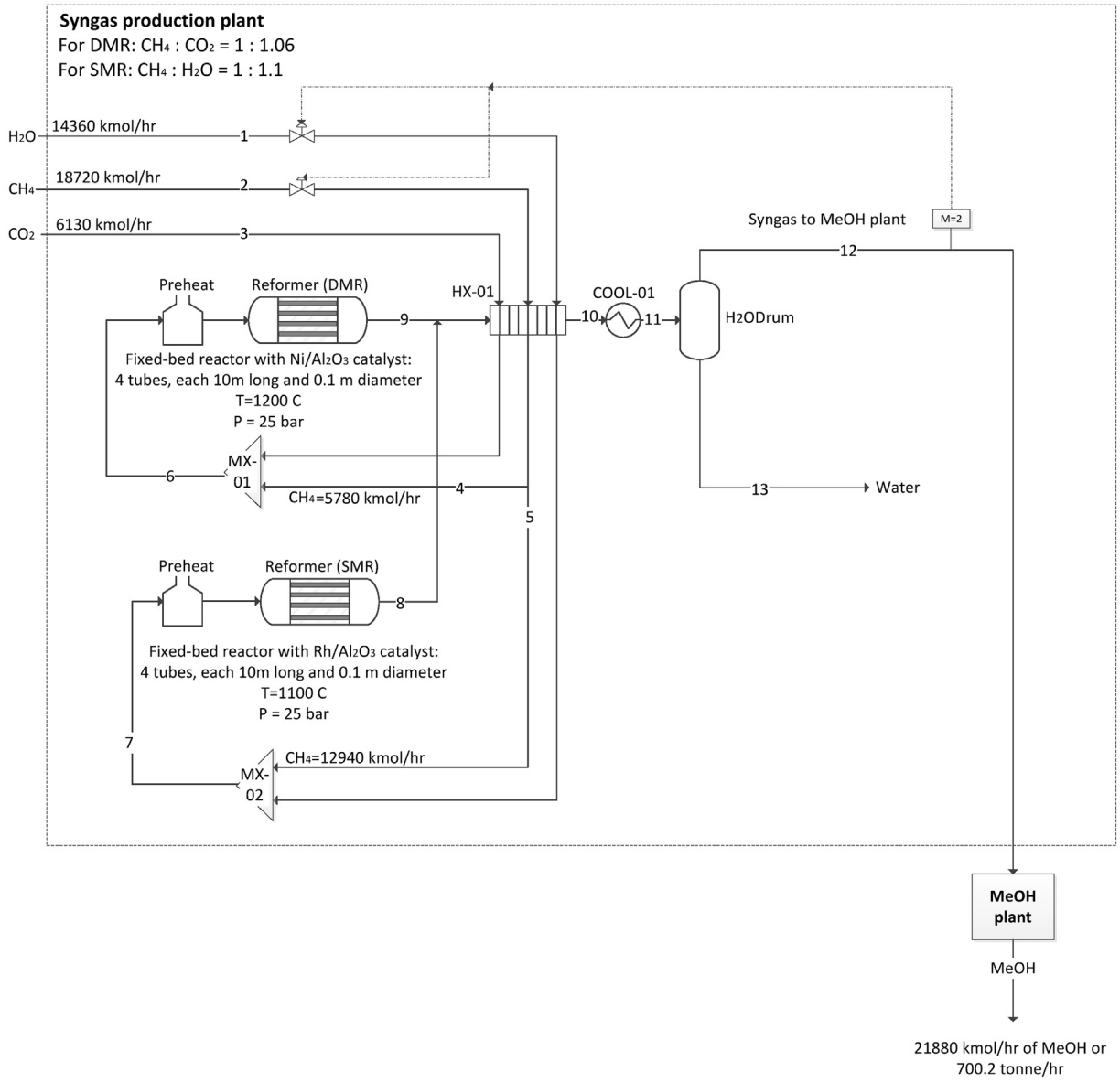

Fig. 11. Process flow diagram for parallel configuration SMR and DMR for the syngas production plant, feed rates to DMR (CH_4—stream 4 and CO_2—stream 3) are fixed at 5780 kmol/h and 6130 kmol/h, respectively while feed rates to SMR (stream 5 and 1) are manipulated to make the stoichiometric *M* in stream 12 equal to 2.

Scenario 4: Parallel SMR & DMR

In this scenario, both SMR and DMR are carried out in parallel reformers, the syngas produced (streams 8 and 9) are then mixed, processed and sent to the MeOH production plant (stream 12) as presented in Fig. 11. In order to produce syngas with stoichiometric number *M* equal to 2, the total methane (stream 2) and water (stream 1) feed rates are manipulated as shown in Fig. 10. The results show that the lowest feed rates for H_2O and CH_4 that can digest the captured CO_2 effectively (to produce *M* equals to 2) are 14,360 kmol/h and 18,720 kmol/h, respectively.

The feeds (CH_4, H_2O and CO_2) are heated by exchanging heat with the syngas mixture from DMR and SMR reformers (streams 8 and 9) in a heat exchanger (HX-01) (Fig. 11). The feed water (14,360 kmol/h) and carbon dioxide (6130 kmol/h) are sent to the SMR and DMR reformers, respectively, while the methane (18,720 kmol/hr) is divided into two streams (4 and 5) that pass to SMR (69.1 mol%) and DMR reformers (30.9 mol%), respectively. The methane flow rate in stream 4 that enters the DMR is fixed at 5780 kmol/h. This is because DMR in this scenario is treated as a standalone reformer, hence the DMR feed rates (CH_4 and CO_2) are similar to Scenarios 1 and 2. The respective feeds for DMR and SMR are preheated up to the reformer temperatures. After giving up heat, the syngas mixture (stream 10) is further processed through a cooler (COOL-01) and knock-out drum (H2ODrum). The final syngas (stream 12) with stoichiometric number *M* equal to 2 is sent to the MeOH synthesis plant.

The two reformers' models (DMR and SMR) are developed and optimized using the RPlug reactor model in Aspen Plus. These

Table 4
Calculated metrics for Scenario 4.

Methane intensity	0.429	$tonne_{CH_4}/tonne_{MeOH}$
CO_2 feed intensity	0.38	$tonne_{CO_{2-feed}}/tonne_{MeOH}$
Energy intensity	13.62[a](0.67)	$GJ_{thermal(electrical)}/tonne_{MeOH}$
CO_2 emission intensity	2.026	$tonne_{CO_2}/tonne_{MeOH}$

[a] For heating (11.3%), cooling (45.8%) and supplying energy to the reformer (42.9%).

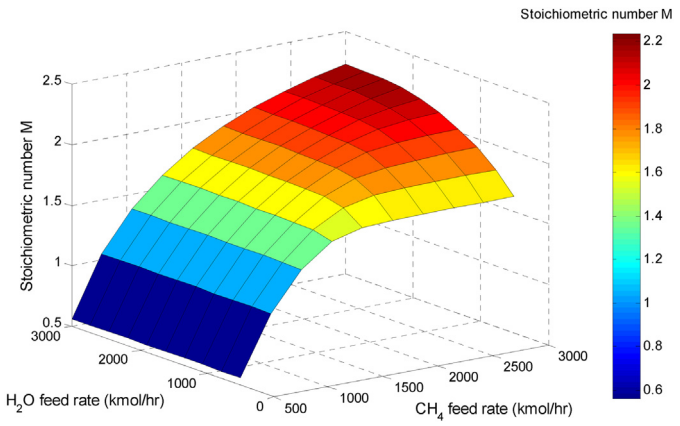

Fig. 12. Variations of stoichiometric M at different CH_4 and H_2O feed rates in Scenario 5.

plug-flow reformers are configured with 10 tubes, each being 10 m in length and 0.1 m in diameter. For DMR reaction, the steady-state kinetics for a Rh/Al_2O_3 catalyst as reported by Richardson and Paripatyadar is used [30]. Whereas the kinetics for a Ni/Al_2O_3 catalyst reported by Xu and Froment are used for SMR reaction [33]. The kinetic expressions reported in those papers are re-arranged into Aspen Plus compatible form for LHHW kinetic.

The MeOH production capacity for this scenario is 700.2 tonne/h which has the same order of magnitude compared to Scenario 3 (using bireforming in the reformer). Using the simulation results summarized in Table 12, the four metrics (Fig. 4) are calculated from Eqs. (5)–(8) and reported in Table 4.

Scenario 5: Simultanous SMR and DMR and PO (trireforming)

In this scenario, three reforming reactions, namely SMR, DMR and PO, are carried out simultaneously in one reactor. The process

Table 5
Calculated metrics for Scenario 5.

Methane intensity	0.435	$tonne_{CH_4}/tonne_{MeOH}$
CO_2 feed intensity	0.333	$tonne_{CO_{2-feed}}/tonne_{MeOH}$
Energy intensity	12.3[a](0.63)	$GJ_{thermal(electrical)}/tonne_{MeOH}$
CO_2 emission intensity	1.93	$tonne_{CO_2}/tonne_{MeOH}$

[a] For heating (9.9%), cooling (48.2%) and supplying energy to the reformer (42%).

flow diagram is shown in Fig. 13 where four feeds (CH_4, H_2O, CO_2 and O_2) enter one reformer. Oxygen is assumed to be supplied from a carbon-free water splitting plant; hence the associated CO_2 emission is negligible. The reformer (with $T = 1200\,^{\circ}C$ and $P = 25$ bar) is modeled using the Gibbs reactor model in Aspen Plus which calculates thermodynamic equilibrium of a process using Gibbs free energy minimization technique. The validity of the Gibbs reactor in predicting trireforming results has been shown in Song and Pan. The authors performed experimental study of trireforimg on Ni-based catalyst with various supports (e.g., MgO, Mg–CeZrO, Al_2O_3), respectively, at atmospheric pressure and temperature range 700 °C to 850 °C [34]. At low temperatures (below 800 °C), deviations between experimental and thermodynamic-predicted results are large (10% for CH_4 conversion and 30% for CO_2 conversion); while at higher temperatures (above 850 °C), the deviations seem to be less (5% and 10% for CH_4 and CO_2 conversions, respectively) [34]. Moreover, since trireforimg is a relatively new technology, to the best of our knowledge, complete reaction kinetics are currently unavailable in the literature. Recent publications related to the modeling aspect of trireforimg include the work from Farniaei et al. [35]. In that study, Farniaei et al. developed a comprehensive model for a packed-bed trireformer. For SMR and DMR reactions, the authors used steady-state kinetics on a Ni catalyst reported by Xu and Froment [33], while for

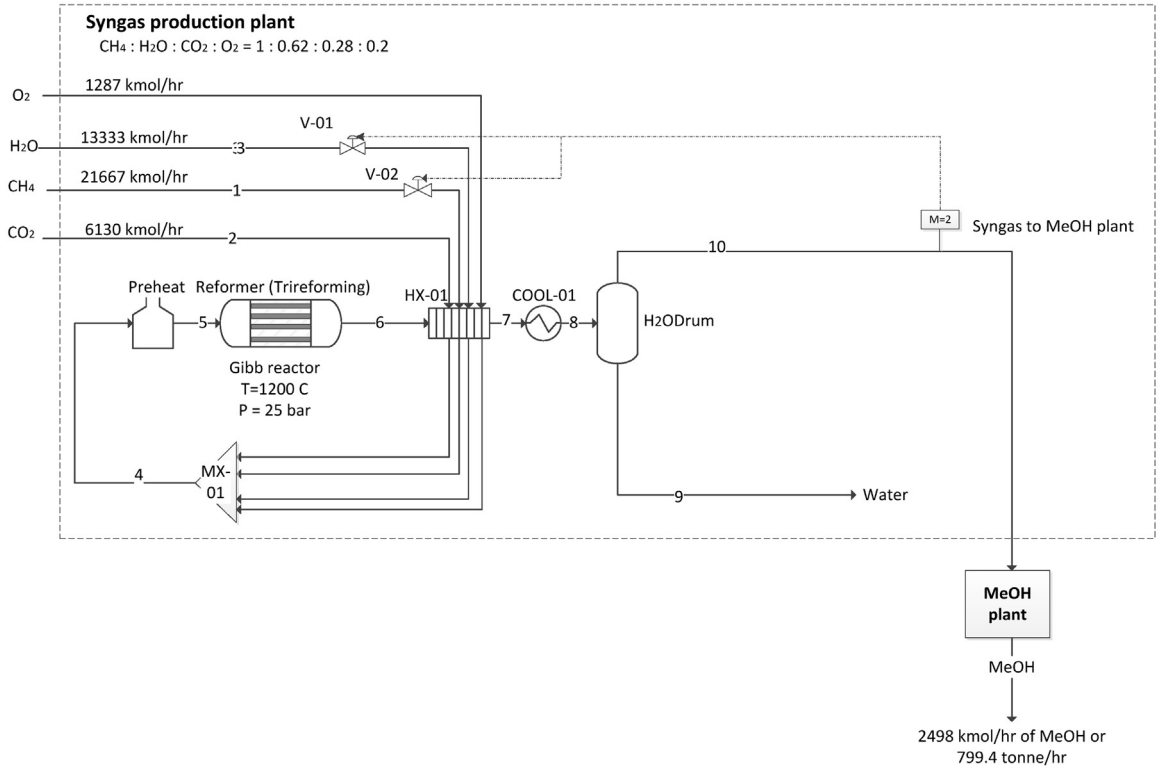

Fig. 13. Process flow diagram for syngas production plant using trireforming technology, feed rate of CH_4 and H_2O are manipulated while the molar ratio O_2: CO_2 is fixed at 0.21 in order to produce syngas (stream 10) with M equal to 2.

Table 6
Metrics calculated from simulation result reported in Milani et al. for CO_2 utilization in MeOH using syngas produced by SMR.

Methane intensity	0.44	$tonne_{CH_4}/tonne_{MeOH}$
CO_2 feed intensity	0.347	$tonne_{CO_{2-feed}}/tonne_{MeOH}$
Energy intensity	11.46[a] (0.64)	$GJ_{thermal(electrical)}/tonne_{MeOH}$
CO_2 emission intensity	1.909	$tonne_{CO_2}/tonne_{MeOH}$

[a] For heating (13.3%), cooling (42.9%) and reformer duty (46.8%).

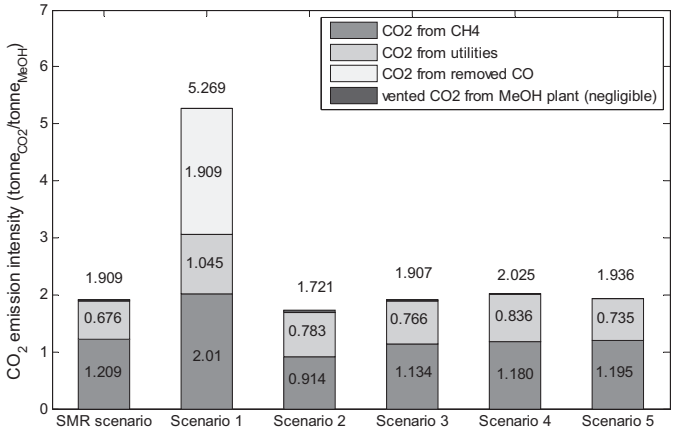

Fig. 14. Summary of CO_2 emission intensity for all scenarios.

Table 7
Cooling and reformer duty required to produce 1 t of MeOH in each scenario computed from the energy intensity reported in Table 1–6.

Scenario	Cooling duty ($GJ/tonne_{MeOH}$)	Reformer duty ($GJ/tonne_{MeOH}$)
SMR	4.91	5.36
1 (Outlier)	5.98	9.63
2	6.15	5.25
3	5.39	5.84
4	6.24	5.85
5	5.92	5.15

Table 8
CO_2 emission intensity when the cooling duty (GJ/tonne MeOH) between scenarios are levelized, in this table we used the cooling duty of base scenario (4.913 GJ/t MeOH) to replace cooling duty in other scenarios.

Scenario	CO_2 emission intensity ($tonne_{CO_2}/tonne_{MeOH}$)
SMR	1.909
1 (Outlier)	5.091
2	1.582
3	1.858
4	1.951
5	1.861

methane total oxidation, the kinetics for a Pt-based catalyst reported in Trimm and Lam [36] were modified to be compatible with a Ni-based catalyst. Unfortunately, the PO reaction, which is an essential reaction path for producing heat, CO and H_2, was not included in Farniaei et al. [35]. Because of this lack in the literature, the Gibbs reactor model in Aspen Plus is used to simulate the reformer in this scenario.

The molar ratio between O_2 and CO_2 feed rates is fixed at 0.21 for good conversion of CO_2 as suggested by Song and Pan [34]. This also aids to reduce the number of degrees of freedom to 2 (i.e., only need to manipulate the CH_4 and H_2O feeds rate to make the stoichiometric number *M* equals to 2). Increasing O_2 flow rate will have minor effect on H_2/CO ratio (i.e., 'M'), while increasing the cost to supply pure O_2 [37]. Hence, given the captured CO_2 is 6130 kmol/h, the feed rate for O_2 is 1287 kmol/h. The required oxygen stream is assumed to be supplied from carbon-free source, thus the associated CO_2 emission is negligible.

Flow rates of CH_4 (stream 1) and H_2O (stream 3) are sensitized and the results show the minimal feed rate required for CH_4, H_2O to make *M* equals to 2 are 21,667 kmol/h and 13,333 kmol/h, respectively (Fig. 12). MeOH production capacity in this scenario is about 799.4 tonne/h with the consumptions of 347.5, 240.1 and 41.2 tonne of CH_4, H_2O and O_2 per hour, respectively. Performing calculations for metrics as in previous scenario by using the summarised simulation results in Table 13, the results are reported in Table 5.

SMR scenario

This scenario is based on CO_2 utilization for MeOH production using SMR as reported by Milani et al. Milani et al. studied CO_2 utilization for MeOH production using SMR and reported a significant CO_2 abatement (21.9%) in comparison with BAU scenario where PP and MeOH plants work independently [12]. The process flow diagram for this scenario is similar to Scenario 3 (bireforming) (Fig. 9), except the CO_2 stream in the SMR scenario does not involve in syngas production but instead it is mixed with syngas leaving the reformer. Both water and methane feed rate were manipulated to yield the syngas (after mixing with CO_2) to produce stoichiometric number M equal to 2 [12]. The reported simulation results are used to compute the four key metrics, namely methane intensity, CO_2 feed intensity, energy intensity and CO_2 emission intensity, (using Eqs. (5)–(8)) and reported in Table 6.

5. Discussions

5.1. CO_2 emission intensity

In this discussion, the CO_2 emission intensity between all scenarios (five proposed scenarios and SMR scenario) are compared in order to determine the most environmental-friendly scenario. The reported CO_2 emission intensity metric ($tonne_{CO2}/tonne_{MeOH}$) for all scenarios (Tables 1–6) are graphically illustrated in Fig. 14. In the result for each scenario, there are three sources of CO_2e emission contribution coming from: (1) the use of CH_4, (2) utilities, and (3) unreacted CO_2 (or vented CO_2). However, the amount of unreacted CO_2 is always insignificant (less than 1%) compared to other CO_2 contributors. In addition, for Scenario 1 specifically, there is equivalent CO_2e emission from the removed

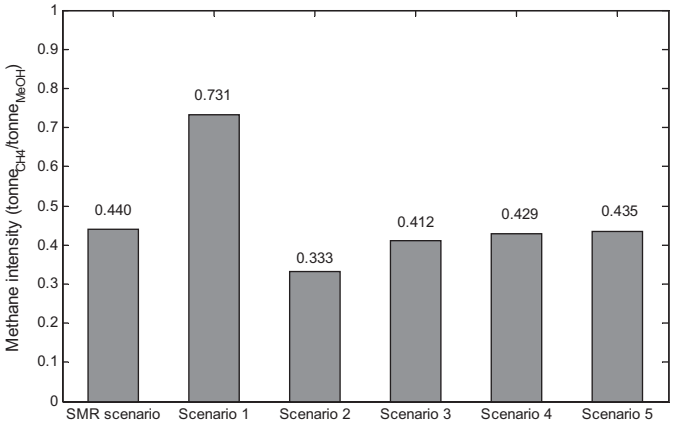

Fig. 15. Comparison of methane CH_4 intensity between scenarios.

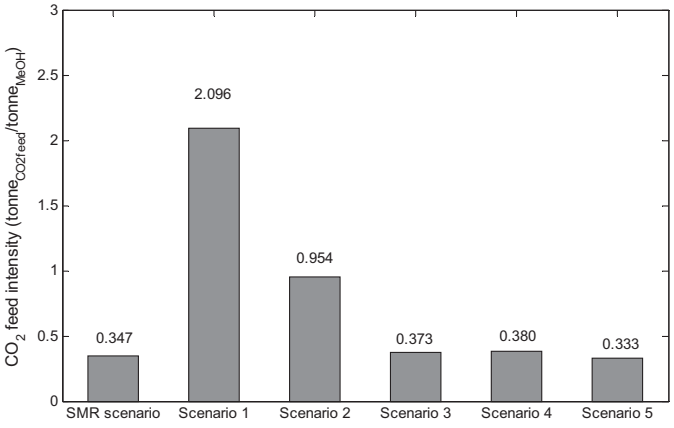

Fig. 16. Comparison of CO_2 feed between scenarios.

CO-rich stream (recalling in Scenario 1, surplus CO is removed to make the stoichiometric number *M* equal to 2). From Fig. 14, it can be seen that Scenario 1 is the 'worst' process as its CO_2 emission intensity is almost four folds compared to other scenarios. This is because in Scenario 1, approximately 54% of the input C atoms (from CO_2 and CH_4) are removed which is equivalent to about 6279 kmol of CO per hour. Given the flow rate of utilized (captured) CO_2 is 6130 kmol/h, overall none of the C atoms in the captured CO_2 are utilized, although it is not necessary that the C atom in the removed CO stream to have originated from captured CO_2. Therefore, even though having similar CCU–MeOH production configuration, Scenario 1 does not demonstrate the benefit of CCU. As a result, it is considered to be an invalid for further discussion.

Examination of other scenarios (SMR and 2–5) shows that Scenario 2 (DMR with H_2 addition) outperforms others by emitting 12.7% less CO_2 on average compared to SMR scenario and Scenarios 3–5. From Fig. 14, although all DMR-based Scenarios (2–5) have the CO_2 emission associated with CH_4 consumption smaller compared to SMR scenario, only Scenario 2 clearly outperforms SMR scenario. This result can be explained by examining the CO_2 contributions from the two sources, these being the utilities (heating, cooling, reformer duty) and CH_4 feed. DMR-based scenarios require less CH_4 to produce a given amount of MeOH in comparison with the SMR scenario (Table 2–6) (in line with Reactions (a) and (b). Therefore, the CO_2 emission intensity contributed from CH_4 in DMR-based Scenarios (2–5) are less than in SMR scenario (−24%, −6%, −2% and −1%, respectively). Furthermore, DMR-based scenarios required higher cooling duty to deal with the higher operating temperature in the reformer or/and higher energy input to drive the reforming reactions as can be seen in Table 7. Heating and electrical duties are found to be similar between scenarios, thus they do not contribute to variations in the CO_2 emission intensities. Subsequently, in those Scenarios (2–5), the CO_2e emissions from utilities are higher in comparison with the SMR scenario (16%, 13%, 24% and 9%, respectively). Therefore, the improved CO_2 emission from consuming less CH_4 in DMR-based scenarios is off-set by the extra CO_2 that comes from higher utility duties. As a result, only Scenario 2, with 'sufficient' saved CO_2 emission from reducing CH_4 uptake, can outperform SMR scenario. In other words, the 'environmental' benefit of Scenario 2 from reducing CH_4 uptake is partially recognized, whereas in DMR derivative Scenarios (3–5) this benefit is completely outweighed by the extra CO_2 emission from higher utilities energy consumption.

In Table 7, it can be seen that variations in cooling duties is the main reason that causes the utilities consumption (and the associated CO_2 emission) in Scenario 2–5 to be higher compared to the SMR scenario. This finding suggests that potentially with process optimization and catalyst development (to reduce reforming temperature), one can levelize the cooling duty between Scenarios 2–5 and the SMR scenario. If this is achievable, the benefit of DMR-based scenarios from consuming less CH_4 (thus resulting in less associated CO_2 emission) can be fully recognized. In other words, not only Scenario 2 but Scenarios 3–5 might also result in less CO_2 emission compared to SMR scenario. As shown in Table 8, it can be seen that if one can make the cooling duty of Scenarios 2–5 similar to SMR scenario, then in addition to Scenario 2, Scenario 3 (bireforming) and 4 (trireforming) result in about 3% less CO_2 emission compared to SMR scenario.

In summary, Scenario 1 can be considered to generate an outlier result since the removal of surplus CO results in very inefficient CO_2 utilization. Scenario 2 (DMR with H_2 addition) is found to result in the least CO_2 emission intensity per tonne of MeOH produced (emitted on average 12.7% less CO_2 compared to other Scenarios (3–5 and SMR)). For DMR derivative processes (Scenario 3–5), although they consume less CH_4 compared to SMR scenario (i.e., less CO_2 emission from CH_4), they require higher cooling duty to deal with higher operating temperature in the reformers or/and higher thermal duty to drive the reforming reactions. The overall result is the CO_2 emission intensity saved from consuming less CH_4 is outweighed by the extra CO_2 associated with consuming more utilities' duty (mostly cooling purposes). However, it is shown that the saved CO_2 emission of DMR derivatives (Scenarios 3–5) might be recognized once their cooling duty is reduced by potential process optimization and catalyst developments (to reduce reforming reaction temperature).

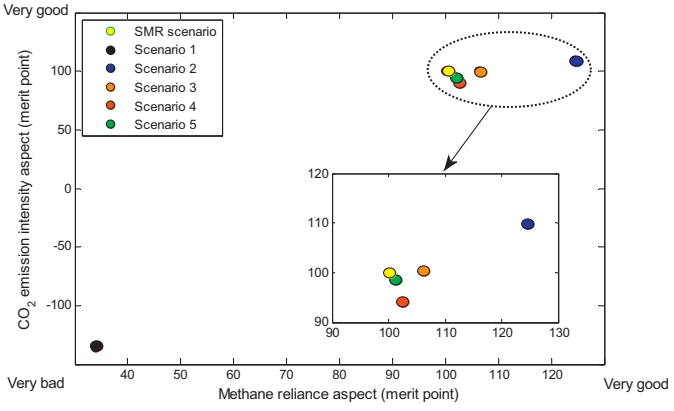

Fig. 17. The overall comparison between scenarios based on two aspects, namely CO_2 emission intensity and methane reliance (equal weights are given to both aspects).

5.2. The extent of methane reliance for MeOH production

As mentioned in the introduction section, the purpose for a transition scheme of the 'methanol economy' is that it needs to be able to partially reduce the reliance on methane in MeOH production as well as mitigating harmful effects from rapid CO_2 emission rates. In this discussion, the extent of methane reliance of each Scenarios (1–5 and SMR) is compared.

From Tables 1–6, the methane intensity ($tonne_{CH4}$/$tonne_{MeOH}$) for Scenario 1 to 5 and the SMR scenario are graphically shown in Fig. 15. Uniquely, Scenario 1 is found to consume the most amount of CH_4 (approximately two folds compared to the other scenarios). This is expected because in Scenario 1 the only source of hydrogen is from CH_4 whereas in other scenarios, hydrogen can come from CH_4, H_2O and even pure H_2 (as in Scenario 2). Therefore, to produce a same amount of MeOH, Scenario 1 will require the highest amount of CH_4. Fig. 16 shows the results for CO_2 feed intensity for

Table 9
Results from mass and energy balance of MeOH production section for Scenario 1 (DMR plant with the alternation of CO partial pressure to give stoichiometric M equal to 2).

	Material flow (tonne/h)	Utilities (GJ/h)	CO_2e emission[a] (tonne/h)
CH_4 feed	92.7	–	255
CO_2 feed	265.9	–	0
Methanol produced	126.8	–	–
CO_2 vented	5	–	5
Removed CO	175.8	–	276.3
Thermal duty[a]	–	2113	127.5
Electrical duty	–	93.1	5.1
CO_2 emitted from MeOH production[c]	–	–	668.9

[b]For heating (6%), cooling (36%) and supplying energy to the reformer (58%) (excluding energy from heat integrations).
[a] CO_2e emission from CH_4 (or CO_2e(3)) = 2.75 × (CH_4 feed rate) (Eq. (3)); For this scenario, there is extra CO_2e emission source which is from the removed CO, this CO2e = 1.75 × (CO flow rate) where '1.75' means by combusting 1 tonne of CO, 1.75 tonne of CO_2 will be emitted. Other CO_2e sources (e.g., thermal duty) are taken from Aspen Plus (assuming process fuel is NG).
[c] Calculated using Eq. (3) (summing all numbers in the 'CO_2e emission column').

Table 10
Results from mass and energy balance for Scenario 2 (DMR plant with the addition of hydrogen to give stoichiometric M equal to 2).

	Material flow (tonne/h)	Utilities (GJ/h)	CO_2 emission[a] (tonne/h)
CH_4 feed	92.7	–	255
CO_2 feed	265.9	–	0
H_2 feed	25.4	–	0
Methanol produced	278.8	–	–
CO_2 vented	6.44	–	6.44
Thermal duty[b]	–	3444	202
Electrical duty	–	292.1	16
CO_2 emitted from MeOH production[c]	–	–	479.4

[a] CO_2e emission from CH_4 (or CO_2e(3)) = 2.75 × (CH_4 feed rate) (Eq. (3)); Other CO_2e sources (e.g., thermal duty) are taken from Aspen Plus (assuming process fuel is NG).
[b] For heating (7.5%), cooling (50%) and supplying energy to the reformer (42.5%) (excluding energy from heat integrations).
[c] Calculated using Eq. (3) (summing all numbers in the 'CO_2e emission column').

Table 11
Results from mass and energy balance for Scenario 3 (using bireforming to produce syngas with stoichiometric M equal to 2).

	Material flow (tonne/h)	Utilities (GJ/h)	CO_2 emission[a] (tonne/h)
CH_4 feed	294.1	–	809
CO_2 feed	265.9	–	0
H_2O feed	259	–	–
Methanol produced	713.3	–	–
CO_2 vented	5.03		5.03
Thermal duty[b]	–	8848	521
Electrical duty	–	444.7	25
CO_2 emitted from MeOH production[c]	–	–	1360

[a] CO_2e emission from CH_4 (or CO_2e(3)) = 2.75 × (CH_4 feed rate) (Eq. (3)); Other CO_2e sources (e.g., thermal duty) are taken from Aspen Plus (assuming process fuel is NG).
[b] For heating (9.5%), cooling (43.5%) and supplying energy to the reformer (47.1%) (excluding energy from heat integrations).
[c] Calculated using Eq. (3) (summing all numbers in the 'CO_2e emission column').

Table 12
Results from mass and energy balance for Scenario 4 (using parallel SMR and DMR to produce syngas with stoichiometric *M* equal to 2).

	Material flow (tonne/h)	Utilities (GJ/h)	CO_2 emission[a] (tonne/h)
CH_4 feed	300.3	–	826
CO_2 feed	265.9	–	0
H_2O feed	258	–	–
Methanol produced	700.2	–	–
CO_2 vented	7	–	7
Thermal duty[b]	–	9538	559
Electrical duty	–	468.8	27
CO_2 emitted from MeOH production[c]	–	–	1419

[a] CO_2e emission from CH_4 (or CO_2e(3)) = 2.75 × (CH_4 feed rate) (Eq. (3)); Other CO_2e sources (e.g., thermal duty) are taken from Aspen Plus (assuming process fuel is NG).
[b] For heating (11.3%), cooling (45.8%) and supplying energy to the reformer (42.9%) (excluding energy from heat integrations).
[c] Calculated using Eq. (3) (summing all numbers in the 'CO_2e emission column').

each scenario reported in Tables 1–6. It can be seen that Scenario 1 consumes CO_2 more than three folds compared to other scenarios. This is because the removal of surplus CO results in not all of the input C atoms being converted into MeOH. As a result, as in CO_2 emission intensity aspect, Scenario 1 can be said to be an outlier from the resources (CO_2 and CH_4) uptake point of view, thus is not included in further discussion.

Table 13
Results from mass and energy balance for Scenario 5 (using trireforming to produce syngas with stoichiometric *M* equal to 2).

	Material flow (tonne/h)	Utilities (GJ/h)	CO_2 emission[a] (tonne/h)
CH_4 feed	347.5	–	955.6
CO_2 feed	265.9	–	0
H_2O feed	240.1	–	–
O_2 feed	41.2	–	0
Methanol produced	799.4	–	–
CO_2 vented	4.6	–	4.6
Thermal duty[b]	–	9809	559
Electrical duty	–	505.8	27
CO_2 emitted from MeOH production[c]	–	–	1546.1

[a] CO_2e emission from CH_4 (or CO_2e(3)) = 2.75 × (CH_4 feed rate) (Eq. (3)); Other CO_2e sources (e.g., thermal duty) are taken from Aspen Plus (assuming process fuel is NG).
[b] For heating (9.9%), cooling (48.2%) and supplying energy to the reformer (42%) (excluding energy from heat integrations).
[c] Calculated using Eq. (3) (summing all numbers in the 'CO_2e emission column').

From Fig. 16, since Scenario 1 is an outlier, Scenario 2 shows to consume the highest amount of utilized CO_2 per tonne MeOH produce which is desirable. Except for Scenario 1 (an outlier as discussed), other Scenarios (3–5 and SMR) have similar CO_2 feed intensities with maximum deviation being 9.5 % (based on SMR scenario value). From the perspective of reducing methane uptake, more utilized CO_2 consumed means less CH_4 demanded for MeOH production. This is because for example: to produce 1 mol of MeOH, 1 mol of C atoms are needed. Hence, if more CO_2 is used, less CH_4 will be needed (so the total C atoms will be 1 mol) and vice versa.

Scenario 2 (DMR with H_2 addition) is found to consume the least amount of methane (22% less on average compared to SMR and ScenarioS 3–5) which is more desirable because of less carbon resource uptake. One possible explanation for the 'very good' methane intensity of Scenario 2 is by considering the source of oxygen in MeOH molecules. As the oxygen source in MeOH molecules produced in Scenario 2 is only contributed by CO_2 molecules, whereas in the other Scenarios (3–5 and SMR) it comes from H_2O, CO_2 and even pure O_2 (in Scenario 5) molecules. Therefore, to synthesize a given amount of MeOH, Scenario 2 will require the highest flow of CO_2. Recalling the relationship 'more input utilized CO_2—less methane required', thus can explain the 'very good' methane intensity of Scenario 2. The consumption of CH_4 between other Scenarios (3–5 and SMR) are similar with maximum deviation is 6% (based on SMR scenario value).

5.3. Overall comparison between scenarios

The results shown in Fig. 14 (CO_2 emission intensity aspect) and Fig. 15 (methane reliance aspect) are combined and presented using a so-called 'merit point' system developed in this section. The calculations of merit points are done by using SMR scenario as a base scenario and assigning it with 100 merit points for each aspect. In this work, equal weight points of 1 are given to the two aspects in calculating the overall merit of each scenario. The weight points can be modified to reflect the different policies in monitoring CO_2 emission or local plant situation (e.g., the availability of NG). For other Scenarios (1–5), the merit points in each aspect are respectively calculated by determine the 'gain' or 'reduction' from 100 merit points of SMR scenario. For example, the CO_2 emission intensity of Scenario 2 is 9.8% less than SMR scenario, thus the merit points given to Scenario 2 for the CO_2 emission intensity aspect is [1 × (100 + 9.8% × 100)] 109.8, where '1' is the weight point. Performing similar calculations for Scenarios 1–5, the overall result are presented in Fig. 17. It can be seen that there are four groups of scenario that are ranked from 'very good to very bad' on both aspects, namely (group 1) Scenario 2; (group 2) Scenario 3; (group 3) Scenarios 4, and 5 and SMR; (group 4) Scenario 1. Scenario in group 4 is obviously not a good choice because it performs badly. Scenarios in group 3 only slightly underperform compared to scenario in group 2. However, in order to determine the 'best' scenario in group 3, further evaluations, e.g., economic aspect, is required which is beyond the scope of this work. Overall, both scenarios in group 1 and 2, i.e., Scenarios 2 and 3, seemed to be very promising candidates.

While Scenario 2 (DMR with H_2 addition) significantly outperforms other Scenarios (1–5 and SMR), its draw-back for practical applications is the requirement for carbon-free hydrogen as well as catalyst deactivation issue due to coke formation [17]. On the other hand, Scenario 3 (bireforming) although it comes as a second-best scenario, its outlook is arguably more promising compared to Scenario 2 due to its ability in significantly mitigate coke formation [38] as well as eliminating the need for carbon-free H_2. Moreover, there are recent developments on bireforming catalysts suitable for commercialization purpose [39]. Although, catalysts used in DMR are still under R&D, plausible progresses have been made in developing novel catalysts [16–19]. Nevertheless, placing Scenarios 2 and 3 into the context of transition strategy for 'methanol economy' (Fig. 1), Scenario 2 could have furthest sustainable MeOH production (i.e., 100% carbon-free) because it consumes the least amount of CH_4 and requires carbon-free H_2 supplied from carbon-free water splitting plant. This hydrogen requirement will potentially create incentive for R&D to drive the development of a sustainable carbon-free hydrogen sector to provide sufficient carbon-free hydrogen for novel global MeOH production [15]. Whereas, in Scenario 3 (bireforming) H_2 in H_2O is extracted by supplying heat (i.e., from NG combustion) into the reformer, thus it still depends extensively on fossil fuel. In summary, Scenario 2 is the most suitable process to apply during MeOH production transitional stage from carbon-based to carbon-free methodology.

6. Conclusion

In this paper, a CCU based MeOH production was studied in which the captured CO_2 from a PCC plant (265.9 tonne/h) is co-fed with methane into the reformer to produce syngas suitable for MeOH synthesis. This MeOH production practice partially reduced the demand on CH_4, thus it is suitable to apply during transitional stage of the 'methanol economy'. Five scenarios using this CCU–MeOH scheme with different reforming methodologies were proposed as follows: (1) DMR with surplus CO removal; (2) DMR with H_2 addition; (3) Bireforming; (4) Parallel SMR and DMR; (5) Trireforming. In addition, a SMR–MeOH from Milani et al. configured similar to the studied CCU scheme was included in the comparison between scenarios [12]. A comprehensive model for each scenario was developed in Aspen Plus. Sensitivity tests were performed to determine the feed flow rates (CH_4, H_2O) to produce syngas with a stoichiometric number *M* equals to 2. For comparison purposes, simulation results for each scenario were used to compute four metrics, namely methane intensity, CO_2 feed intensity, energy intensity and CO_2 emission intensity. These

metrics were used to evaluate and compare between scenarios from two aspects, the CO_2 emission intensity and methane reliance.

In both aspects, Scenario 1 (DMR with surplus CO removal) was considered irrelevant for comparison since it did not demonstrate the benefits of CO_2 utilization (reduction in CO_2 emission and methane uptake) due to the CO removal mechanism. Scenario 2 (DMR with H_2 addition) significantly outperformed other scenarios by 12.7% and 22% on average, respectively. The reduction in CO_2 emission intensity in Scenario 2 versus other scenarios was found to originate from the savings in methane uptake. Currently, practical applications of Scenario 2 are likely to be challenged by technical issues (e.g., catalyst deactivation due to coke formation) and the current status of carbon-free H_2 sector. However, in intermediate term, Scenario 2 will be the most suitable process to apply during the transitional stage of MeOH production from carbon-based to carbon-free methodology in accordance with the 'methanol economy'.

References

[1] IPPC, summary for policymakers, in: O. Edenhofer, R. Pichs-Madruga, Y. Sokona, E. Farahani, S. Kadner, K. Seyboth, A. Adler, I. Baum, S. Brunner, B. Eickemeier, J. Savolainen, S. Schlomer, C.V. Stechow, T. Zwickel, J.C. Minx (Eds.), Climate Change, 2014, Mitigation of Climate Change, Cambridge University Press, Cambridge, United Kingdom and New York, NY, USA, 2014 (Chapter 6).

[2] CIA, The World Factbook 2014.

[3] G.A. Olah, A. Goeppert, G.K.S. Parakas, Beyond Oil and Gas: The Methanol Economy, Wiley, 2009.

[4] G.A. Olah, A. Goeppert, G.K.S. Prakash, Chemical recycling of carbon dioxide to methanol and dimethyl ether: from greenhouse gas to renewable, environmentally carbon neutral fuels and synthetic hydrocarbons, J. Org. Chem. 74 (2009) 487–498.

[5] J. Kim, C.A. Henao, T.A. Johnson, D.E. Dedrick, J.E. Miller, E.B. Stechel, C.T. Maravelias, Methanol production from CO_2 using solar thermal energy: process development and techno-economic analysis, Energy Environ. Sci. 4 (9) (2011) 3122–3132.

[6] N. von der Assen, P. Voll, M. Peters, A. Bardow, Life cycle assessment of CO2 capture and utilization: a tutorial review, Chem. Soc. Rev. 43 (23) (2014) 7982–7994.

[7] E.S. Van-Dal, C. Bouallou, CO_2 abatement through a methanol production process, Chem. Eng. Trans. 2012 (2012) 29.

[8] M. Pérez-Fortes, A. Bocin-Dumitriu, E. Tzimas, CO_2 utilization pathways: techno-economic assessment and market opportunities, Energy Procedia 63 (2014) 7968–7975.

[9] IAEA, IAEA Nuclear Energy Series. 2013.

[10] J. Fletcher, V. Roan, D. Betts, An investigation of the feasibility of coal-based methanol for application in transportation fuel cell systems 3rd International Energy Conversion Engineering Conference, (2005) California 2005.

[11] P. Galindo Cifre, O. Badr, Renewable hydrogen utilisation for the production of methanol, Energy Convers. Manage. 48 (2) (2007) 519–527.

[12] D. Milani, R. Khalilpour, G. Zahedi, A. Abbas, A model-based analysis of CO2 utilisation in methanol synthesis plant, J. CO_2 Util. 10 (2015) 12–22.

[13] G.A. Olah, A. Goeppert, M. Czaun, G.K.S. Prakash, Bi-reforming of methane from any source with steam and carbon dioxide exclusively to metgas ($CO–2H_2$) for methanol and hydrocarbon synthesis, J. Am. Chem. Soc. 135 (2013) 648–650.

[14] I. Dushyant Shekhawat, J.J. Spivey, I.A. David Berry (Eds.), Fuel Cells: Technologies for Fuel Processing, Elsevier, 2011.

[15] O.O. James, S. Maity, M.A. Mesubi, K.O. Ogunniran, T.O. Siyanbola, S. Sahu, R. Chaubey, Towards reforming technologies for production of hydrogen exclusively from renewable resources, Green Chem. 13 (2011) 2272–2284.

[16] X.E. Verykios, Catalytic dry reforming of natural gas for the production of chemicals and hydrogen, Int. J. Hydrogen Energy 28 (2003) 1045–1063.

[17] J. Newnham, Optimisation and characterisation of nickel based nano-catalysts for the dry reforming of methane with carbon dioxide, Appl. Sci. RMIT (2012) .

[18] S. Tungkamani, M. Phongaksorn, P. Narataruksa, T. Sornchamn, N. Kanjanabat, N. Siri-Nguan, Developing carbon tolerance catalyst for dry methane reforming, Chem. Eng. Trans. 2013 (2013) 32.

[19] E. Lovell, Y. Jiang, J. Scott, F. Wang, Y. Suhardja, M. Chen, J. Huang, R. Amal, CO_2 reforming of methane over MCM-41-supported nickel catalysts:altering support acidity by one-pot synthesis at room temperature, Appl. Cata. A: Gen. 473 (2014) 51–58.

[20] B. Lima, O. Araújo, J.L.C. Medeiros Morgado, Technical, economic and environmental viability of offshore CO_2 reuse from natural gas by dry reforming, Carbon Dioxide Capture Technologies and Its Use, Marriott Marquis & Hilton, Atlanta, GA, 2014 14AIChE.

[21] P. Biedermann, T. Grube, H. Bernd, Methanol as an energy carrier, Forschungszentrum Zentralbibliothek (2006) .

[22] R.C. Brown, in: R.C. Brown (Ed.), Thermochemical Processing of Biomass: Conversion into Fuels, Chemicals and Power, vol. 12, Wiley, 2011, pp. 348.

[23] R. Agrawal, N.R. Singh, F.H. Ribeiro, W.N. Delgass, Sustainable fuel for the transportation sector, Proc. Natl. Acad. Sci. 104 (12) (2007) 4828–4833.

[24] G.A. Olah, G.K.S. Prakash, Conversion of carbon dioxide to methanol using bi-reforming of methane or natural gas, Google Patents (2008) .

[25] H. Er-rbib, C. Bouallou, F. Werkoff, Production of synthetic gasoline and diesel fuel from dry reforming of methane, Energy Procedia 29 (2012) 156–165.

[26] A.J. Majewski, J. Wood, Tri-reforming of methane over Ni@SiO_2 catalyst, Int. J. Hydrogen Energy 39 (24) (2014) 12578–12585.

[27] N.v.d. Assen, J. Jung, A.e. Bardow, Life-cycle assessment of carbon dioxide capture and utilization: avoiding the pitfalls, Energy Environ. Sci. 2013 (2013) 6.

[28] W. Wu, W. Felicia, and H.-T. Yang, Optimization of Syngas Production Systems Subject to Almost Net-zero CO_2 Emission, ADCONP, Editor. 2014.

[29] E.S. Van-Dal, C. Bouallou, Design and simulation of a methanol production plant from CO_2 hydrogenation, J. Clean. Prod. 57 (2013) 38–45.

[30] J.T. Richardson, S.A. Paripatyadar, Carbon dioxide reforming of methane with supported rhodium, Appl. Catal. 61 (1990) 293–309.

[31] P.J. Robinson, Dynamic modeling and plantwide control of a hybrid power and chemical plant: an integrated gasification combined cycle coupled with a methanol plant, Chem. Eng. Lehigh University (2011) .

[32] P. Shahkarami, Mathematical modeling and optimization of combined steam and dry reforming of methane process in catalytic fluidized bed membrane reactor, Chem. Eng. Commun. 202 (6) (2015) .

[33] J. Xu, G.F. Froment, Methane steam reforming, methanation and water-gas shift: I. Intrinsic kinetics, AIChE J. 35 (1998) 88–96.

[34] C. Song, W. Pan, Tri-reforming of methane: a novel concept for synthesis of industrially useful synthesis gas with desired H_2/CO ratios using CO_2 in flue gas of power plants without CO_2 seperation in ACS, Div. Fuel Chem. (2004) .

[35] M. Farniaei, M. Abbasi, H. Rahnama, M.R. Rahimpour, A. Shariati, Syngas production in a novel methane dry reformer by utilizing of tri-reforming process for energy supplying: modeling and simulation, J. Nat. Gas Sci. Eng. 20 (2014) 132–146.

[36] D.L. Trimm, C.W. Lam, The combustion of methane on platinum–alumina fibre catalysts I: kinetics and mechanism, Chem. Eng. Sci. 6 (1980) 1405–1413.

[37] W. Pan, Tri-reforming and combined reforming of methane for producing syngas with desired H_2/CO ratios, in Department of Materials Science and Engineering, Pennsylvania State University, 2002.

[38] L.C.S. Kahle, T. Roussière, L. Maier, K.H. Delgado, G. Wasserschaff, S.A. Schunk, O. Deutschmann, Methane dry reforming at high temperature and elevated pressure: impact of gas-phase reactions, Ind. Eng. Chem. Res. 52 (2013) 11920–11930.

[39] S.S. Itkulova, G.D. Zakumbaeva, Y.Y. Nurmakanov, A.A. Mukazhanova, A.K. Yermaganbetova, Syngas production by bireforming of methane over Co-based alumina-supported catalysts, Catal. Today 228 (2014) 194–198.